TECHNICAL NOTE:

ASSESSING CLIMATE CHANGE IMPACT ON HYDROLOGICAL COMPONENTS OF A SMALL FOREST WATERSHED THROUGH SWAT CALIBRATION OF EVAPOTRANSPIRATION AND SOIL MOISTURE

H.-K. Joh, J.-W. Lee, M.-J. Park, H.-J. Shin, J.-E. Yi, G.-S. Kim, R. Srinivasan, S.-J. Kim

ABSTRACT. *This study evaluates the future impact of climate change on hydrological components in a 8.54 km^2 mixed forest watershed located in the northwest of South Korea. Before future assessment, the SWAT (Soil Water Assessment Tool) model was calibrated using two years (2007-2008) and validated by using one year (2009) of daily observed streamflow, evapotranspiration, and soil moisture. Hydrological predicted values matched well with the observed values during calibration and validation ($R^2 \geq 0.6$ and Nash-Sutcliffe efficiency ≥ 0.5). The MIROC3.2hires GCM (general circulation model) data of the SRES (special report on emissions scenarios) A1B and B1 scenarios of the IPCC (Intergovernmental Panel on Climate Change) were adopted for future assessment and downscaled using the LARS-WG (Long Ashton Research Station - Weather Generator) stochastic weather generator after bias correction with 30 years (1970-2000) of ground measured data. The A1B scenario reflects a future world of very rapid economic growth, low population growth, and rapid introduction of new and more efficient technology. The B1 scenario reflects a very heterogeneous world. The underlying theme is that of strengthening regional cultural identities, with an emphasis on family values and local traditions, high population growth, and less concern for rapid economic development. As a result, the future changes in annual temperature, precipitation, and evapotranspiration showed an upward tendency and streamflow and soil moisture showed a downward tendency in both scenarios.*

Keywords. *A1B scenario, B1 scenario, Climate change, Evapotranspiration, Mixed forest, Soil moisture, SWAT.*

Fossil fuel consumption has caused an increase in anthropogenic emissions of carbon dioxide (CO_2) and other greenhouse gases (IPCC, 2007). Due to higher concentrations of these gases in the atmosphere, the proportion of solar radiation hitting the Earth that is reflected back into space is reduced, leading to a net warming of the planet (Kalnay and Cai, 2003). The magnitude of this increase will depend on future human activities; however, all IPCC (2007) scenarios have predicted that increases in atmospheric greenhouse gas concentrations will raise surface temperatures.

These changes will likely affect the hydrologic cycle (Fricklin et al., 2009). Recently, a number of studies on the impact of climate on runoff have been performed that have coupled GCM (general circulation model) outputs with the SWAT model. Jha et al. (2004) studied the impacts of climate change on streamflows in the Mississippi River watershed using SWAT. Gosain et al. (2006) assessed the hydrology affected by climate change in Indian river watersheds using SWAT. Zhang et al. (2007) used SWAT to simulate the impacts of climate change on the streamflows in a Chinese river basin. Ficklin et al. (2009) examined the climate change sensitivity assessment of an agricultural watershed using SWAT model. Ficklin et al. (2010) assessed the sensitivity of agricultural streamflow load to rising levels of CO_2 and climate change in the San Juan Valley watershed in California. Park et al. (2010) assessed the future impact of climate change on hydrological behavior considering future vegetation canopy prediction and its propagation to nonpoint-source pollution (NPS) loads using SWAT in a forest-dominant watershed in South Korea.

In many cases of SWAT calibration and validation, streamflow was the single most commonly used watershed response variable (Arnold and Allen, 1996; Manguerra and Engel, 1998; Peterson and Hamleet, 1998; Sophocleous et al., 1999). However, as the SWAT models have been developed to reflect spatially distributed information about watersheds, e.g., elevation, soil, and land use, model calibration

Submitted for review in October 2010 as manuscript number SW 8877; approved for publication as a Technical Note by the Soil & Water Division of ASABE in June 2011.

The authors are **Hyung-Kyung Joh, ASABE Member,** Graduate Student, Department of Rural Engineering, and **Ji-Wan Lee, ASABE Member,** Graduate Student, **Min-Ji Park,** Post-Doctoral Researcher, and **Hyung-Jin Shin,** Post-Doctoral Researcher, Department of Civil and Environmental System Engineering, Konkuk University, South Korea; **Jae-Eung Yi,** Professor, Department of Environmental and Urban System Engineering, Ajou University, Suwon, South Korea; **Gwang-Seob Kim,** Professor, Department of Civil Engineering, Kyungpook National University, Daegu, South Korea; **Ragahavan Srinivasan, ASABE Member,** Professor, Spatial Science Laboratory, Department of Ecosystem Sciences and Management, Texas A&M University, College Station, Texas; and **Seong-Joon Kim, ASABE Member,** Professor, Department of Civil and Environmental System Engineering, Konkuk University, Seoul, South Korea. **Corresponding author:** Seong-Joon Kim, Department of Civil and Environmental System Engineering, Konkuk University, 1 Hwayang-dong, Gwangjin-gu, 143-701 Seoul, South Korea; phone: +82-2-450-3749; e-mail: kimsj@konkuk.ac.kr.

  ISSN 2151-0032

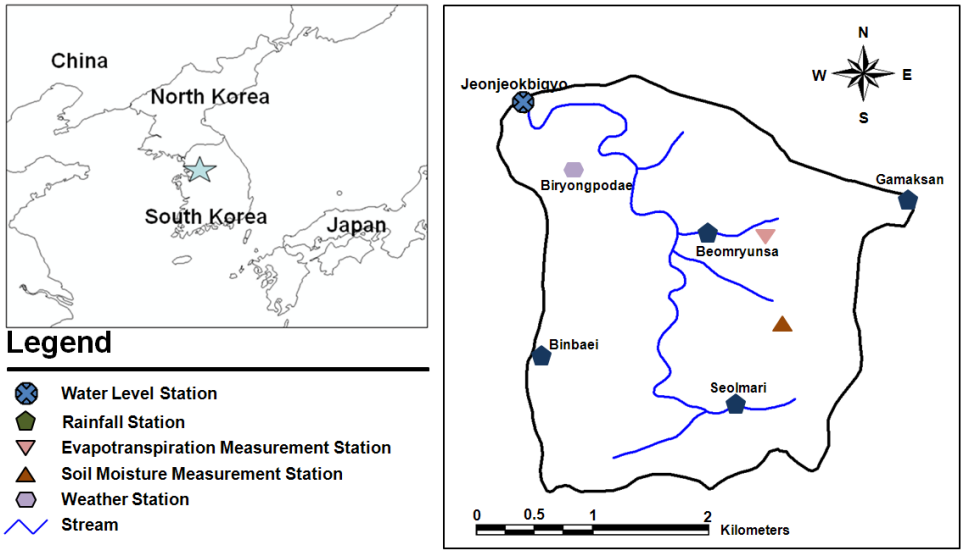

Figure 1. Location and gauge stations of the study watershed.

has become possible with measured state variables in addition to measured streamflow. Until now, few experiments and/or current measures for multivariable calibration have been tried, and future strategies for the adaptation of hydrological component changes as a result of climate change are needed.

Accordingly, this study evaluates the impact of future climate change on the hydrologic components of a small, forest-dominant watershed using the spatially calibrated (using measured evapotranspiration and soil moisture in addition to streamflow) SWAT model. The MIROC3.2hires GCM data are prepared for the watershed by LARS-WG (Long Ashton Research Station - Weather Generator) downscaling. For the 2040s and 2080s SRES A1B and B1 scenarios, the SWAT model projects the climate change impact on future watershed hydrology.

Material and Method

SWAT Model Description

SWAT is a physically based, continuous-time, conceptual, long-term, distributed-parameter model designed to predict the effects of land management practices on the hydrology, sediment, and contaminant transport in agricultural regions. The watershed is subdivided into subbasins based on the number of tributaries. The size and number of subbasins are variable, depending on the stream network and the size of the entire watershed. Each subbasin is further disaggregated into classes of hydrological response units (HRUs), whereby each unique combination of the underlying geographical maps (soils, land use, etc.) forms one class (Ullrich and Volk, 2009). The hydrologic components (e.g., streamflow, evapotranspiration, soil moisture, etc.), sediment, and nutrient loadings from each HRU are calculated and predicted separately using input data about weather, soil properties, topography, vegetation, and land management practices and then summed together to determine the total loadings from the subbasin (Neitsch et al., 2001a). The hydrologic routines within SWAT account for vadose zone processes (i.e., infiltration, evaporation, plant uptake, lateral flows, and percolation), and groundwater flows. The hydrologic cycle as simulated by SWAT is based on the water balance equation:

$$SW_t = SW_0 + \sum_{i=1}^{t} \left(R_{day} - Q_{surf} - E_a - W_{seep} - Q_{gw} \right) \quad (1)$$

where SW_t is the final soil water content (mm H_2O), SW_0 is the initial soil water content on day i (mm H_2O), t is the time (d), R_{day} is the amount of precipitation on day i (mm H_2O), Q_{surf} is the amount of surface runoff on day i (mm H_2O), E_a is the amount of evapotranspiration on day i (mm H_2O), W_{seep} is the amount of water entering the vadose zone from the soil profile on day i (mm H_2O), and Q_{gw} is the amount of return flow on day i (mm H_2O).

Study Watershed Description

The forest-dominant Seolma-Cheon watershed (8.54 km^2) was adopted as the study area. Figure 1 shows the location within the latitude-longitude range of 37° 55′ 25″ N to 37° 56′ 50″ N and 126° 55′ 30″ E to 126° 57′ 30″ E, and the gauge stations for rainfall, weather, streamflow, evapotranspiration, and soil moisture. The watershed average elevation and slope are 247.8 m and 2.00%, respectively. The land use consists of 88.1% forest, 4.6% upland crop, 2.2% urban area, and 5.1% pasture and bare field. The dominant soil is sandy loam (76.4%). The annual average precipitation in the watershed is 1210.0 mm, and the mean temperature is 10.3°C over the last ten years (2000-2009). This watershed is very steep, and the water level appears to increase sharply after a crushing zone is filled by precipitation (Korea Institute of Construction Technology, http://kict.datapcs.co.kr/new-main.htm).

GIS, RS, Meteorological, and Measured Data

The SWAT model basically requires elevation, land use, soil, and meteorological data at desired locations in the watershed. Figure 2 shows the elevation, land use, and soil information for the study watershed. The elevation data were rasterized to 30 m resolution from a vector map of 1:5,000 scale that was supplied by the Korea National Geography In-

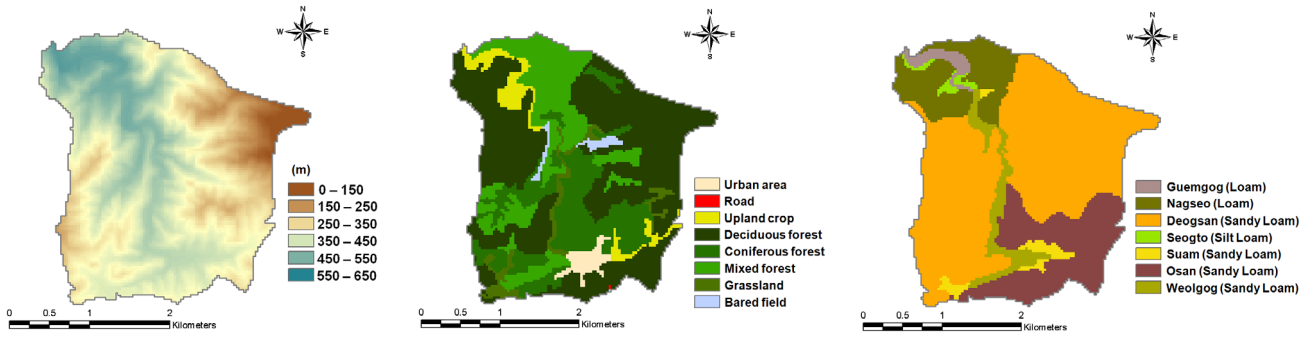

(a) DEM **(b) Land use** **(c) Soil**

Figure 2. GIS and RS data for the study watershed.

Table 1. Data sets for SWAT model parameterization.

Data Type	Source	Scale or Period	Data Description
Topography	Korea National Geography Institute	30 m	Digital elevation model (DEM)
Soil	Korea Rural Development Administration	1:25,000	Soil classification and physical properties, e.g., texture, porosity, field capacity, wilting point, saturated conductivity, and depth.
Land use	2004 Landsat TM satellite image	1:25,000	Landsat land use classification (eight classes).
Weather	Korea Institute of Construction Technology, Water Management Information System	2007-2009	Daily precipitation, minimum and maximum temperature, mean wind speed and relative humidity data.
Streamflow	Korea Institute of Construction Technology, Yonsei University	2007-2009	Daily streamflow data at watershed outlet.
Soil moisture	Korea Institute of Construction Technology, Yonsei University	2007-2009	Bihourly soil moisture data at mixed forest and sandy loam area.
Evapotranspiration	Korea Institute of Construction Technology, Yonsei University	2007-2009	Daily evapotranspiration data at mixed forest area.

stitute. The soil information was from a 1:25,000 vector map that was supplied by the Korea Rural Development Administration. The land use was prepared by classifying Landsat TM satellite images (3 June 2004). The HRUs were created using the spatial information.

Daily meteorological data were collected for three years (2007-2009) from one weather station and four rainfall stations (fig. 1). The mean, maximum, and minimum temperature (˚C), precipitation (mm), relative humidity (%), wind speed (m s^{-1}), and sunshine hours (h) were prepared for Penman-Monteith ET calculation. Two years and seven months (June 2007 to December 2009) of daily soil moisture (SM), two years and four months (September 2007 to December 2009) of evapotranspiration (ET), and three years (2007-2009) of daily streamflow (Q) were prepared for model calibration and validation. The data measurement was managed by the Korea Institute of Construction Technology and Department of Atmospheric Sciences, Yonsei University, Korea.

As shown in figure 1, the soil moisture was measured with a TDR (time domain reflectometry) system buried in the sandy loam of a mixed forest area at 10, 30, and 60 cm depths from the surface, and evapotranspiration was measured with an eddy covariance system at the upper part of a mixed forest. The eddy covariance system was set on top of a 20 m tower that is over twice the height of the vegetation (9 m). Table 1 shows the sources of the input and measured data.

Climate Change Scenarios and GCM Data

The IPCC has published a set of emission scenarios in the SRES (Special Report on Emissions Scenarios; Nakicenovic et al., 2000) to serve as a basis for assessments of future climate change. Among the SRES scenarios, four marker scenarios (A1, A2, B1, and B2) are by far the most often used (Van Vuuren and O'Neill, 2006; fig. 3.). The A1 and B1 scenarios emphasize the ongoing globalization and project future worlds with less difference between regions, while the A2 and B2 scenarios emphasize the regional and local social economic and environmental development and project more differential worlds. The A1 scenario develops into three groups that describe alternative directions of technological change in the energy system. The three A1 groups are distinguished by their technological emphasis: fossil intensive (A1Fi), non-fossil energy sources (A1T), and a balance across all sources (A1B). The regionally downscaled A1B and B1 scenarios were adopted in this study. Under the A1B and B1 scenarios, the GHGs (greenhouse gases) and other gases and driving forces were quantified in the IPCC's Fourth Assessment Report (IPCC, 2007) for use in climate simulation by GCMs (Park et al., 2009).

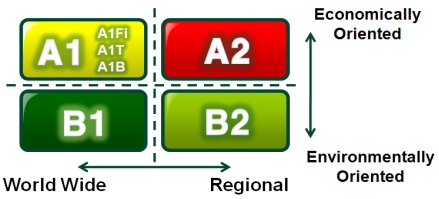

Figure 3. Four markers of emission scenarios.

GCM Data and Downscaling Method

As GCM data, the MIROC3.2hires data from two SRES climate change scenarios (A1B and B1) developed by the National Institute for Environmental Studies of Japan were adopted from the IPCC Data Distribution Center (www.mad.zmaw.de/IPCC_DDC/html/SRES_AR4/index.html). Here, A1B is a "middle" GHGs emission scenario and B1 is a "low" GHG emission scenario.

The MIROC3.2hires GCM data were downscaled by two steps for the study watershed. As the first step, to ensure that the historical data (30 years of data from 1971 to 2000) and GCM output have similar statistical properties, the bias-correction method described by Alcamo et al. (1997) was used. This method is generally accepted within the global change research community (IPCC, 1999). For temperature, absolute changes between historical and future GCM time slices were added to measured values:

$$T'_{GCM,fut} = T_{GCM,fut} + (\overline{T}_{meas} - \overline{T}_{GCM,his}) \quad (2)$$

where $T'_{GCM,fut}$ is the transformed future temperature, $T_{GCM,fut}$ is the original future GCM temperature, $\overline{T}_{meas}$ is the average measured temperature for the 30-year baseline period, and $\overline{T}_{GCM,his}$ is the average historical GCM temperature. For precipitation, relative changes between historical data and GCM output were applied to measured historical values:

$$P'_{GCM,fut} = P_{GCM,fut} \cdot (\overline{P}_{meas} / \overline{P}_{GCM,his}) \quad (3)$$

where $P'_{GCM,fut}$ is the transformed future precipitation, $P_{GCM,fut}$ is the original future GCM precipitation, $\overline{P}_{meas}$ is the average measured precipitation, and $\overline{P}_{GCM,his}$ is the average historical GCM precipitation.

Secondly, daily rainfall amount and minimum (T_{min}) and maximum (T_{max}) daily temperatures were estimated over 100-year simulated periods using the LARS-WG stochastic weather generator. LARS-WG was chosen over WXGEN, the weather generator included in SWAT, so that the generated data could be manipulated for climate change scenarios before SWAT input. LARS-WG was also found to produce better precipitation and minimum and maximum temperature results for diverse climates than other weather generators (Semenov et al., 1998). LARS-WG is based on the weather series generator described by Racsko et al. (1991). It utilizes semi-empirical distributions for the lengths of wet and dry day series, and daily precipitation. Daily minimum and maximum temperatures are considered as stochastic processes, with daily means and daily standard deviations depending on the wet or dry status of the day (Ficklin et al., 2009). LARS-WG is widely used for climate change studies (e.g., Semenov and Barrow, 1997; Semenov et al., 1998). Input data for LARS-WG consisted of CIMIS climate data collected at four weather stations within the study area (fig. 1). The remaining climate data required for SWAT simulation (solar radiation and relative humidity) were generated by the WXGEN weather generator (Sharpley and Williams, 1990) included in SWAT. To address the inconsistencies between the two weather generators, Ficklin et al. (2009) compared generated results for precipitation, minimum and maximum temperature, and solar radiation. The comparisons showed that LARS-WG and WXGEN were both successful at generating climate variables close to the observed values, suggesting that the discrepancies between the two weather generators were minor.

Model Calibration and Validation

Before model calibration and validation, we conducted a sensitivity analysis of the input parameters concerned with streamflow (Q), evapotranspiration (ET), and soil moisture content (SM). To ensure an efficient calibration, a sensitivity analysis was conducted to identify the most sensitive parameters (Kannan et al., 2007). The sensitivity analysis was conducted by the LH-OAT (Latin hypercube - one factor at a time) method, which combines the OAT design with Latin hypercube sampling. Through the LH-OAT method, the dominant hydrological parameters were determined and a reduction of the number of model parameters was performed (van Griensven and Meixner, 2003).

Table 2 shows the selected parameters for the sensitivity analysis and calibrated results. The SCS curve number (CN2)

Table 2. Calibrated SWAT model parameters.

		Bounds[a]				Value Used in Literature		
Parameter	Definition	LB	UB	Sensitivity	Adjusted Value	Zhang et al. (2007)	Muleta and Nicklow (2005)	Galvan et al. (2009)
Streamflow (Q)								
CN2	SCS curve number for moisture condition	35	98	High	0 to +4	-4 to +2	--	-2
Surlag	Surface runoff lag coefficient	1	24	Medium	2.4	--	--	--
GWQMN	Threshold depth of water in the shallow aquifer required for return flow	0	100	High	0	--	--	--
GW_DELAY	Groundwater delay	0	500	High	100	--	--	1
GW_REVAP	Groundwater revap coefficient	0.02	0.2	Medium	0.2	--	--	0.2
Soil moisture (SM)								
ESCO	Soil evaporation compensation factor	0	1	High	0.01	0.4	0.0882	0.01
SOL_AWC	Available water capacity of the soil layer	0	1	High	--	--	--	+0.04
SOL_BD	Moist bulk density	0.9	2.5	High	--	--	--	--
CANMX	Maximum canopy storage	0	100	High	5	--	--	--
Evapotranspiration (ET)								
ESCO	Soil evaporation compensation factor	0	1	High	0.01	0.4	0.0882	0.01
EPCO	Plant uptake compensation factor	0	1	High	1	0.2	1	--
CANMX	Maximum canopy storage	0	100	High	5	--	--	--

[a] LB = lower bound, UB = upper bound.

Table 3. Summary of streamflow for calibration and validation period.[a]

Year	P (mm)	Q (mm) Obs.	Q (mm) Sim.	QR (%) Obs.	QR (%) Sim.	*E*	R^2	Note
2007	1262.2	761.0	748.2	0.60	0.59	0.60	0.65	C
2008	1498.3	941.7	978.4	0.63	0.65	0.80	0.83	C
2009	1351.7	1000.9	920.6	0.74	0.68	0.86	0.88	V
Mean	1387.7	1094.7	999.7	0.74	0.72	0.76	0.78	--

[a] P = precipitation, Q = streamflow, QR = runoff ratio, *E* = Nash-Sutcliffe model efficiency, R^2 = coefficient of determination, C = calibration, and V = validation.

was sensitive to peak flow and amount of discharge. Increasing CN2 by 20% resulted in a 1.4% increase in Q and 5% in peak flow. GW_ DELAY, GW_ REVAP, and Surlag affected the recession phase of hydrograph. A 20% increase in CANMX increased ET by 1.9%. A 20% decrease in ESCO increased ET by 3.8% and decreased SM by 1.7%. EPCO had an inverse relationship with ESCO.

The SWAT model was calibrated using streamflow data measured at the watershed outlet and ET and SM data measured in the mixed forest area. The calibration was carried out using two years (2007 and 2008) of data. The winter soil moisture from December to February could not be observed due to frozen field conditions. Tables 3 and 4 show the summary of two years of calibration results for Q, ET, and SM, and figure 4 shows a comparison of the measured versus simulated Q, ET, and SM. The average coefficient of determination (R^2; Legates and McCabe, 1999) and the Nash-Sutcliffe model efficiency (*E*; Nash and Sutcliffe, 1970) for Q were 0.74 and 0.70, respectively, and the R^2 values for SM and ET were 0.58 and 0.58, respectively.

The model validation was conducted with 2009 Q, ET, and SM data. The results are shown in tables 3 and 4 and figure 4. The R^2 and *E* for Q were 0.76 and 0.71, and the R^2 values for SM and ET were 0.55 and 0.66, respectively. The R^2 value indicates that the observed versus simulated plot was close to 1:1, and *E* indicates that the observed and simulated values were closer (Santhi et al., 2001). A value of 1 indicates that the simulation exactly corresponds to the observed data. During November to March, the differences between the simulated and observed streamflow were very consistent (fig. 4). The differences were within a range of 0.1 to 1 mm. The errors may have resulted from the use of default LAI (leaf area index) values instead of observed or measured LAI. Thus, ET was affected and influenced the streamflow simulation for these periods. If the LAI had been measured, we could have achieved better results. The LAI values could be extracted from satellite images, such as terra MODIS (Moderate Resolution Imaging Spectroradiometer), but the images were too large and rough to be useful. The difference between model performance in the calibration and validation periods is also because the hydrologic conditions in the validation period may have changed and did not exactly resemble the conditions during the calibration period (e.g., Beven, 2006; Liu and Gupta, 2007; Zhang et al., 2009).

Table 4. Statistical summary of soil moisture and evapotranspiration for calibration and validation period.[a]

Year	P (mm)	SM (%) Period	SM (%) Obs.	SM (%) Sim.	ET (mm) Period	ET (mm) Obs.	ET (mm) Sim.	R^2 SM	R^2 ET	Note
2007	1262.2	June-Dec.	13.7	14.0	Sept.-Dec.	109.0	73.1	0.71	0.60	C
2008	1498.3	Jan.-Dec.	11.7	12.8	Jan.-Dec.	471.7	376.9	0.45	0.56	C
2009	1351.7	Jan.-Dec	12.1	14.6	Jan.-Dec.	408.6	395.3	0.55	0.66	V
Mean	1370.7	--	12.5	13.8	--	330.0	281.8	0.55	0.59	--

[a] P = precipitation, SM = soil moisture, ET = evapotranspiration, R^2 = coefficient of determination, C = calibration, and V = validation.

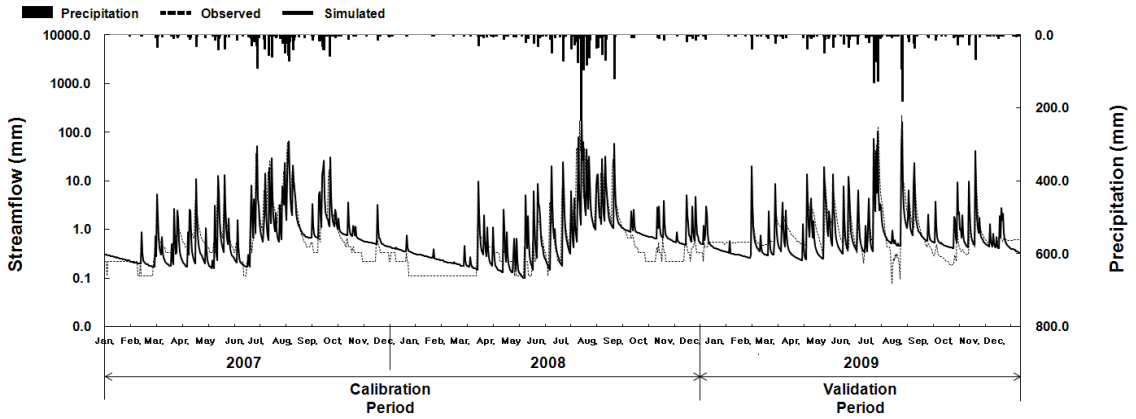

(a) Streamflow

Figure 4. Comparison of the measured versus simulated (a) streamflow, (b) evapotranspiration, and (c) soil moisture averaged in depth (cont'd).

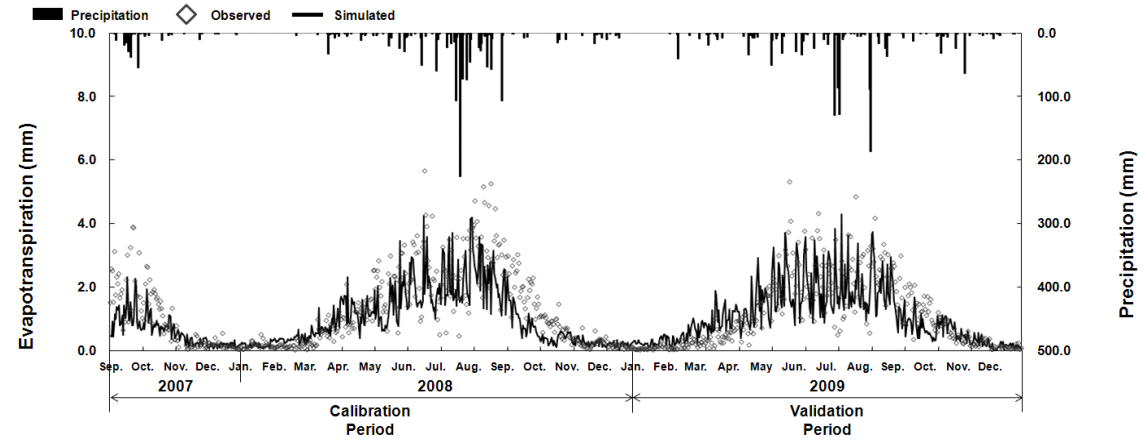

(b) Evapotranspiration

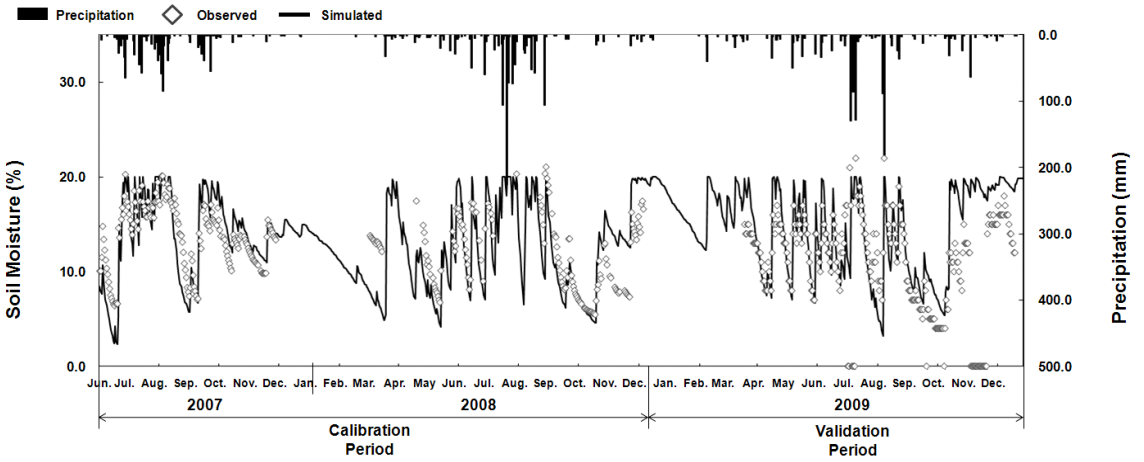

(c) Soil moisture

Figure 4 (cont'd). Comparison of the measured versus simulated (a) streamflow, (b) evapotranspiration, and (c) soil moisture averaged in depth.

Results and Discussions

Climate Change Impacts on Q, ET, and SM

By using the calibrated SWAT model, the future (2040s and 2080s) climate change impacts on the hydrologic components of the study watershed were evaluated with the MIROC3.2hires A1B and B1 downscaled data. Table 5 shows the future projected seasonal temperature (T), precipitation (P), Q, ET, and SM, and figure 5 shows the future monthly P, T, Q, ET, and SM based on the 2009 SWAT-simulated data. The largest increases in future temperature and precipitation were 4.3˚C and 15.3% in the 2080s A1B scenario. The future increase in temperature caused an increase in ET relative to the baseline. The largest annual ET increase was 62.0% (242.4 mm) with a 9.8% (132.4 mm) annual precipitation increase and 3.2˚C annual temperature increase in the 2040s B1 scenario. The temperature increase follows CO_2 increase scenarios. The A1B and B1 scenarios showed a sharp CO_2 emission increase in the near future and am emission decrease in the far future. The CO_2 decrement of the B1 scenario is greater than that of the A1B scenario (fig. 6). This phenomenon similarly affected changes in temperature. Accordingly, the results show that the temperature difference between the baseline (2009) and the 2040s is much greater than the temperature difference between the 2040s and the 2080s.

The future increase in ET successively caused a decrease in SM. The largest annual SM decrease was 38.4% in the 2080s B1 scenario. The effect of future precipitation was subdued by the future temperature. The future streamflow decreased due to the increase in ET and decrease in SM even with the increase in precipitation. The largest decrease in annual streamflow was 18.0% (166.0 mm) in the 2080s B1 scenario, and the largest decrease in seasonal streamflow was 34.3%, which occurred in spring of the 2080s A1B scenario. Meanwhile, the future large increase in rainfall in the autumn season increased the streamflow, with a maximum increase of 130.0% in the 2040s A1B scenario. Thus, it might be necessary to establish policies for use and control of the autumn water resources in the future. Henceforth, as additional future assessment strategies for the changes in hydrologic components due to climate change, methods such as land use change impact or LAI change impact will be explored.

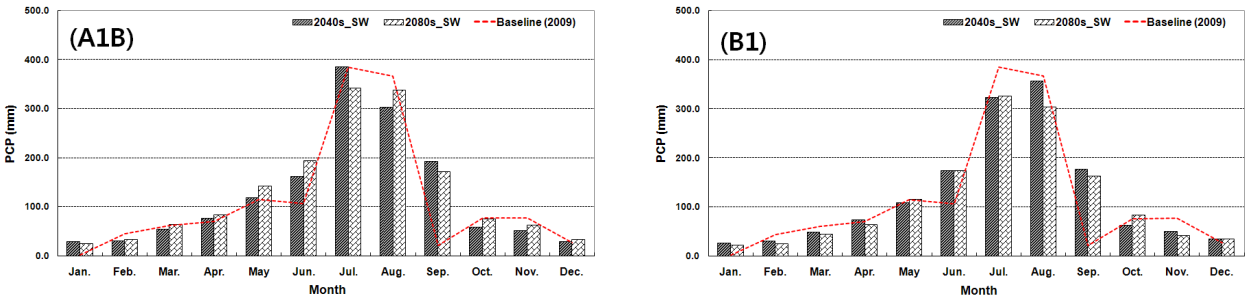

(a) Precipitation

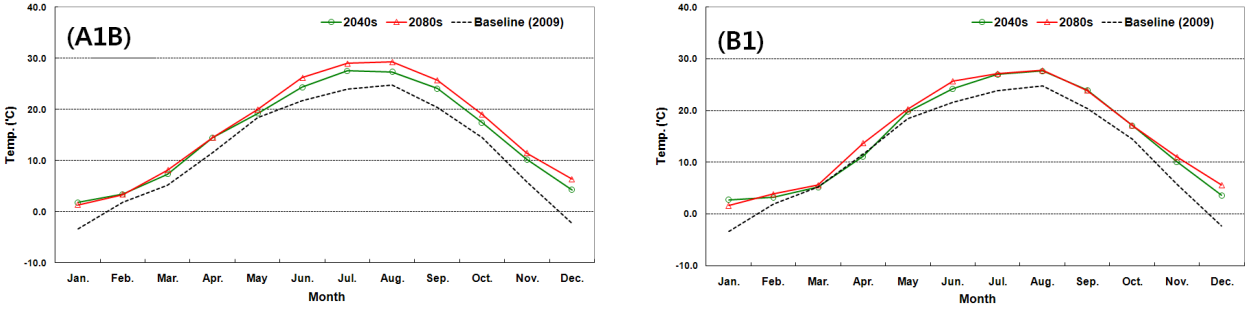

(b) Temperature

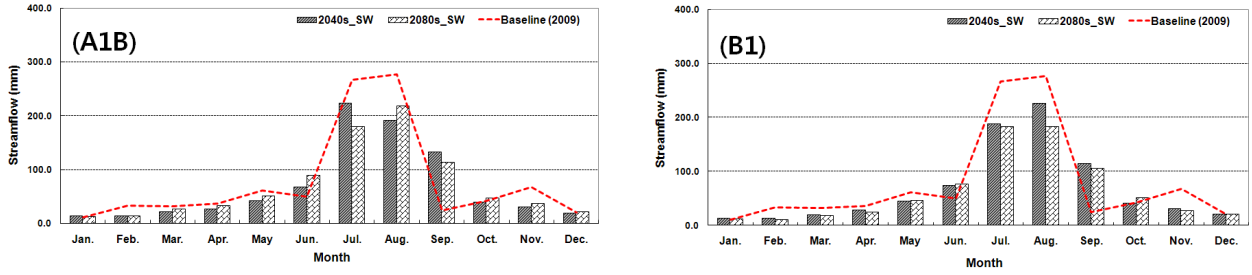

(c) Streamflow

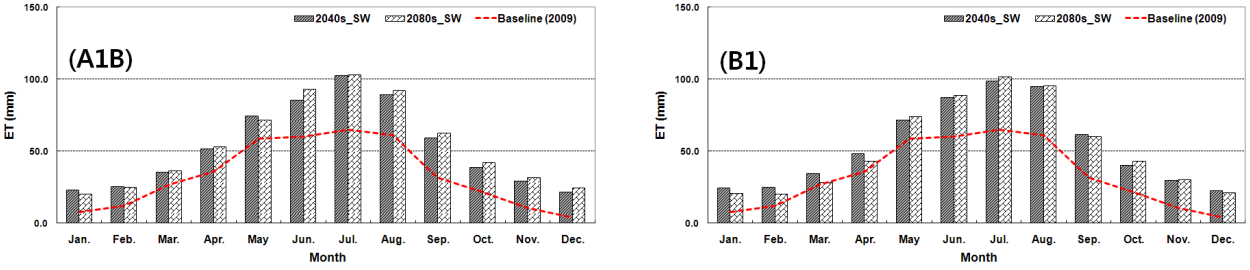

(d) Evapotranspiration

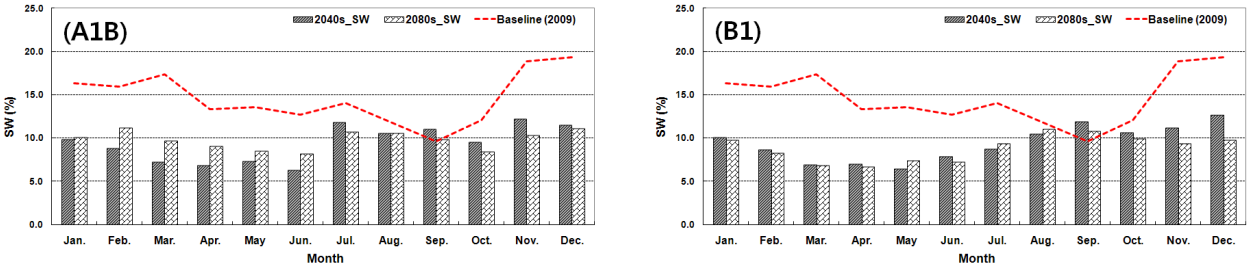

(e) Soil moisture

Figure 5. Future projected monthly (a) precipitation, (b) temperature, (c) streamflow, (d) ET, (e) and SM based on 2009 data.

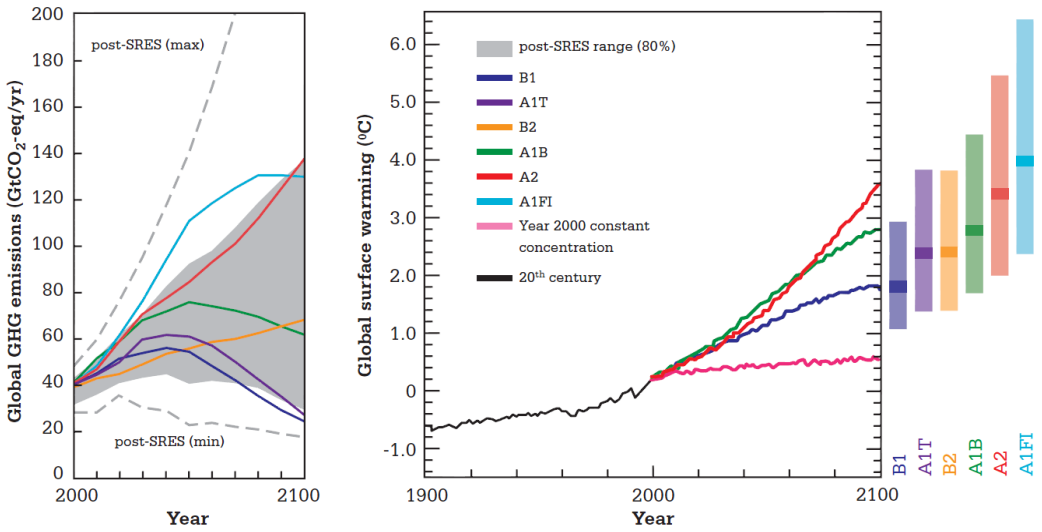

Figure 6. Scenarios for GHG emissions from 2000 to 2100 and estimates of corresponding surface temperatures (WTO, 2009).

Table 5. Change in future temperature (T), precipitation (P), streamflow (Q), evapotranspiration (ET), and soil moisture (SM) values compared to the base year (2009).

Scenario and Period	T (°)	P (%)	Q (%)	ET (%)	SM (%)
A1B Scenario					
2040s					
Winter	+4.4	+452.4	-14.1	+243.4	-42.0
Spring	+1.9	-1.0	-30.6	+34.4	-51.3
Summer	+3.0	+11.5	-3.2	+49.2	-26.1
Autumn	+3.7	+243.2	+130.0	+115.4	-14.2
Annual	+3.2	+9.8	-11.0	+61.3	-34.2
2080s					
Winter	+4.9	+383.6	-23.9	+252.4	-37.3
Spring	+2.5	+15.1	-34.3	+30.5	-38.0
Summer	+4.7	+21.1	-4.7	+47.2	-24.0
Autumn	+5.2	+222.5	+91.0	+102.8	-24.9
Annual	+4.3	+15.3	-16.1	+56.8	-32.9
B1 Scenario					
2040s					
Winter	+4.5	+418.8	-11.5	+256.5	-39.9
Spring	+0.3	-7.1	-30.5	+28.6	-53.6
Summer	+2.9	+14.9	+0.2	+51.4	-29.4
Autumn	+3.5	+220.5	+10.5	+120.2	-10.2
Annual	+2.8	+8.4	-11.9	+62.0	-34.6
2080s					
Winter	+4.9	+338.3	-21.3	+216.2	-46.2
Spring	+1.5	-12.5	-34.1	+17.3	-52.2
Summer	+3.5	+10.6	-3.9	+53.9	-28.1
Autumn	+3.8	+204.7	+100.4	+125.0	-19.3
Annual	+3.4	+3.3	-18.0	+58.9	-38.4
Baseline (2009)[a]	T (°)	P (mm)	Q (mm)	ET (mm)	SM (%)
Winter	-1.3	73.1	99.3	22.6	18.2
Spring	11.7	246.7	101.3	74.87	15.5
Summer	23.5	856.5	377.2	183.7	13.4
Autumn	13.6	175.4	342.9	114.1	11.2
Annual	11.9	1351.7	920.6	395.3	14.6

[a] T is average; P, Q, ET, ad SM are totals.

Summary and Conclusions

This study tried to evaluate the future impact of climate change on hydrological components in a small forest watershed by calibrating SWAT with forest evapotranspiration and soil moisture in addition to streamflow at the watershed outlet. The model calibration (2007-2008) and validation (2009) results had Nash-Sutcliffe model efficiencies of 0.70 and 0.86 for streamflow and R^2 values 0.59 and 0.55 for evapotranspiration and soil moisture.

The future assessment was conducted by using the MIROC3.2hires A1B scenario (middle CHG emission and warming) and B1 scenario (low CHG emission and warming). The monthly data were downscaled at daily scale using the LARS-WG stochastic method. The future projected annual temperature and precipitation both increased, showing 4.3˚C and 15.3% maximum increases in the 2080s A1B scenario. The future estimated maximum changes in streamflow, evapotranspiration, and soil moisture were -18.0% in the 2080s B1, +62.0% in the 2040s B1, and -38.4% in the 2080s B1 scenario, respectively. The result showed that future temperature affected the hydrologic components of the study watershed more than future precipitation. On the other hand, future streamflow increased from 10.5% to 130.0% due to the large increase in rainfall in the autumn season. This kind of information on future quantitative and estimated hydrologic components will allow appropriate decisions on water resource management for a watershed.

Acknowledgements

This work was supported by a National Research Foundation of Korea (NRF) grant funded by the Korea government (MEST) (No. 2010-0029194) and the Mid-Career Researcher Program through an NRF grant funded by MEST (No. 2009-0080745).

References

Alcamo, J., P. Döll, F. Kaspar, and S. Siebert. 1997. Global change and global scenarios of water use and availability: An application of Water GAP 1.0. Report A9701. Kassel, Germany:

University of Kassel, Center for Environmental Systems Research.
Arnold, J. G., and P. M. Allen. 1996. Estimating hydrologic budgets for three Illinois watersheds. *J. Hydrol.* 176(1): 57-77.
Beven, K. J. 2006. A manifesto for the equifinality thesis. *J. Hydrol.* 320: 18-36.
Ficklin, D. L., Y. Luo, E. Luedelin, and M. Zhang. 2009. Climate change sensitivity assessment of a highly agricultural watershed using SWAT. *J. Hydrol.* 374(1-2): 16-29.
Ficklin, D. L., Y. Luo, E. Luedelin, S. E. Gatzke, and M. Zhang. 2010. Sensitivity of agricultural runoff loads to rising levels of CO_2 and climate change in the San Joaquin Valley watershed of California. *Environ. Pollut.* 158(1): 223-234.
Galvan, L., M. Olias, R. Fernandez de Villaran, J. M. Domingo Santos, J. M. Nieto, A. M. Sarmiento, and C. R. Canovas. 2009. Application of the SWAT model to an AMD-affected river (Meca River, SW Spain) estimation of transported pollutant load. *J. Hydrol.* 377(3-4): 445-454.
Gosain, A. K., S. Rao, and D. Basuray. 2006. Climate change impact assessment on hydrology of Indian river basins. *Current Sci.* 90(3): 346-353.
IPCC. 1999. Guidelines on the use of scenario data for climate impact and adaptation assessment, Version 1. T. R. Carter, M. Hulme, and M. Lal, eds. Intergovernmental Panel on Climate Change, Task Group on Scenarios for Climate Impact Assessment. Available at: www.ipcc-data.org/guidelines/TGICA_guidance_sdciaa_v1_final.pdf.
IPCC. 2007. Climate change 2007: The physical science basis. Contribution of Working Group I to the 4th Assessment Report of the Intergovernmental Panel on Climate Change. Cambridge, U.K.: Cambridge University Press.
Jha, M., Z. Pan, E. S. Takle, and R. Gu. 2004. Impacts of climate change on streamflow in the upper Mississippi River basin: A regional climate model perspective. *J. Geophysical Res.* 109(D9): D09105.
Kalnay, E., and M. Cai. 2003. Impact of urbanization and land-use change on climate. *Nature* 423(6939): 528-531.
Kannan, N., S. M. White, F. Worrall, and M. J. Whelan. 2007. Sensitivity analysis and identification of the best evapotranspiration and runoff options for hydrological modeling in SWAT-2000. *J. Hydrol.* 332(3-4): 456-466.
Legates, D. R., and G. J. McCabe. 1999. Evaluating the use of goodness-of-fit measures in hydrologic and model validation. *Water Resources Res.* 35(1): 233-241.
Liu, Y., and V. Gupta. 2007. Uncertainty in hydrologic modeling: Toward an integrated data assimilation framework. *Water Resources Res.* 43(7): W07401.
Manguerra, H. B., and B. A. Engel. 1998. Hydrologic parameterization of watersheds for runoff prediction using SWAT. *J. American Resources Assoc.* 34(5): 1149-1162.
Muleta, M. K., and J. W. Nicklow. 2005. Sensitivity and uncertainty analysis coupled with automatic calibration for a distributed watershed model. *J. Hydrol.* 306(1-4): 127-145.
Nakicenovic N., J. Alcmao, G. Davis, B. de Vries, J. Fenhann, S. Gaffin, K. Gregory, A. Grubler, T. Y. Jung, T. Kram, E. L. La Rovere, L. Michaelis, S. Mori, T. Morita, W. Pepper, H. Pitcher, L. Price, K. Riahi, A. Roehrl, H. H. Ronger, A. Sankovski, M. Schlesinger, P. Shukla, S. Smith, R. Swart, H. van Rooijen, N. Victor, and Z. Dadi. 2000. IPCC special report on emissions scenarios. Cambridge, U.K.: Cambridge University Press.
Nash, J. E., and J. V. Sutcliffe. 1970. River flow forecasting through conceptual models: Part I. A discussion of principles. *J. Hydrol.* 10(3): 283-290.
Neitsch, S. L., J. G. Arnold, J. R. Kiniry, and J. R. Williams. 2001a. *Soil and Water Assessment Tool: Theoretical Documentation, Version 2000*. Draft (April 2001). Temple, Tex.: USDA-ARS Grassland, Soil and Water Research Laboratory and Blackland Research Center.
Park, G. A., H. J. Shin, M. S. Lee, W. Y. Hong, and S. J. Kim. 2009. Future potential impacts of climate change on agricultural watershed hydrology and the adaptation strategy of paddy rice irrigation reservoir by release control. *Paddy Water Environ.* 7(4): 271-282.
Park, M. J., J. Y. Park, H. J. Shin, M. S. Lee, G. A. Park, I. K. Jung, and S. J. Kim. 2010. Projection of future climate change impacts on nonpoint-source pollution loads for a dominant dam watershed by reflecting future vegetation canopy in a Soil and Water Assessment Tool model. *Water Sci. and Tech.* 61(8): 1975-1986.
Peterson, J. R., and J. M. Hamlett. 1998. Hydrologic calibration of the SWAT model in a watershed containing fragipan soils. *J. American Water Resources Assoc.* 34(3): 531-544.
Racsko, P., L. Szeidl, and M. Semenov. 1991. A serial approach to local stochastic weather models. *Ecol. Model.* 57(1-2): 27-41.
Santhi, C., G. Arnold, J. R. Williams, W. A. Dugas, R. Srinivasan, and M. Hauck. 2001. Validation of the SWAT model on a large river basin with point and nonpoint sources. *J. American Water Resources Assoc.* 37(5): 1169-1188.
Semenov, M. A., and E. M. Barrow. 1997. Use of a stochastic weather generator in the development of climate change scenarios. *Climatic Change* 35(4): 397-414.
Semenov, M. A., R. J. Brooks, E. M. Barrow, and C. W. Richardson. 1998. Comparison of the WGEN and LARS-WG stochastic weather generators for diverse climates. *Climate Research* 10(2): 95-107.
Sharpley, A. N, and J. R. Williams. 1990. Erosion/Productivity Impact Calculator: 1. Model documentation. Tech. Bulletin 1768. Washington, D.C.: USDA-ARS.
Sophocleous, M. A., J. K. Koelliker, R. S. Govindaraju, T. Birdie, S. R. Ramireddygari, and S. P. Perkins. 1999. Integrated numerical modeling for basin-wide water management: The case of the Rattlesnake Creek basin in south-central Kansas. *J. Hydrol.* 214(1): 179-196.
Ullrich, A., and M. Volk. 2009. Application of the Soil and Water Assessment Tool (SWAT) to predict the impact of alternative management practices on water quality and quantity. *Agric. Water Mgmt.* 96(8): 1207-1217.
Van Griensven, A., and T. Meixner. 2003. Sensitivity, optimization, and uncertainty analysis for the model parameters of SWAT. In *SWAT2003: Proc. 2nd Intl. SWAT Conf.*, 162-167. TWRI technical report 266. College Station, Tex.: Texas Water Resources Institute.
Van Vurren P. D., and B. C. O'Neill. 2006. The consistency of IPCC's SRES scenarios to recent literature and recent projections. *Climate Change* 75(1-2): 9-46.
WTO. 2009. Trade and climate change. A report by the United Nations Environment Program and the World Trade Organization. Geneva Switzerland: World Trade Organization.
Zhang, X., R. Srinivasan, and F. Hao. 2007. Predicting hydrologic response to climate change in the Luohe River basin using the SWAT model. *Trans. ASABE* 50(3): 901-910.
Zhang, X., F. Liang, R. Srinivasan, and M. van Liew. 2009. Estimating uncertainty of streamflow simulation using Bayesian neural networks. *Water Resources Res.* 45(2): W02403.